

# Chapter 10

## Performance of Frequency Ratio Approach for Mapping of Groundwater Prospect Areas in an Area of Mixed Topography



Subhas Garai and Pulakesh Das

**Abstract** Assessment of groundwater potential zones is important to ensure the sustainable use of limited groundwater resources in dry subtropical regions. The increased freshwater demand for households, irrigation during the drier seasons for multiple cropping, economic development, and industrial use imposing threats to water resources, which may continue under the projected change scenarios. The geospatial analysis allows the integration of several proxy variables in demarcating the groundwater potential zones based on the importance of each factor in a GIS environment. In the current study, we have added a number of spatial layers as land use land cover, vegetation density, slope, altitude, rainfall, soil, geology, geomorphology, hydrogeology, drainage density, lineament density, and aquifer to estimate groundwater potential for the Paschim Medinipur and Jhargram district, West Bengal, India. The frequency ratio (FR) method was applied to derive the groundwater potential zones, indicated well-accepted performance judged by the AUC value of 0.732. The study indicated a higher importance of geomorphology, soil, slope, hydrogeology, and aquifer. The high and moderate groundwater potential zones are identified in around 30.15% and 40% of the area, respectively. These areas are mostly observed in the eastern and northern parts of the study area. Moreover, 25.59% of the total area is identified as lower potential zones, mostly distributed in the western part.

**Keywords** Aquifer · Frequency ratio · Groundwater potential · Jhargram · Paschim Medinipur

---

S. Garai · P. Das (✉)

Department of Remote Sensing & GIS, Vidyasagar University, Mindapore, West Bengal, India

## 10.1 Introduction

Ground water is one of the important sources of the natural freshwater stored in the subsurface geological formations. Alteration in the climate condition and over-exploitation of the groundwater for various purposes causing a significant reduction in the groundwater level. The increased demand for groundwater for households, agriculture irrigation, and industrial use imposes an immense pressure on the groundwater resources. The scarcity of groundwater is more severe in the drier sub-tropical, arid, and semi-arid regions with high population density and cropping intensity. Moreover, the regions with intense and recurrent drought events cause degradation in the groundwater level (Pandey and Srivastava 2019). Significant depletion in groundwater resources imposes threats to agricultural productivity and water security. About 68% of the annual groundwater recharge in India is dependent on the rainfall, and another 32% is contributed by the other resources as canal seepage, excess water from cropland, recharge from tanks, ponds, and water conservation structures (Groundwater Yearbook 2013–14). In India, around 62% of the water used in irrigation is extracted from groundwater, while around 85% and 45% of rural and urban water use are extracted from the groundwater resources, respectively (Saha and Ray 2019). According to a study conducted in India's groundwater indicated that more than 54% of the total geographic area experiences high to extremely high water stress (WRI India report 2015). The reduction in precipitation has shown a direct and indirect impact on the groundwater storage, indicated the rate of reduction by  $2 \text{ cm}\cdot\text{year}^{-1}$  and increase by  $1\text{--}2 \text{ cm}\cdot\text{year}^{-1}$  in northern and southern India, respectively, during the period 2002–2013 (Asoka et al. 2017).

The occurrence and distribution of groundwater are primarily regulated by surface and sub-surface soil's porosity and permeability with the underlying lithology (Shahid et al. 2000). The groundwater potentiality is decided based on the different lithology and geomorphic units. The percolation of rainwater, different water channels, and resources through the soil is stored in porous soils and rocks. When the soil zone becomes saturated, water percolates downward. A zone of saturation occurs where all the interstices are filled with water. Groundwater is also recharged when there is a leakage in water supply systems and a surplus of water in agricultural land. Groundwater is stored in the aquifer's zone, which is a geological formation consisting of permeable material capable to store/yield significant quantities of water. Aquifers are composite of unconsolidated sands and gravels, permeable sedimentary rocks (e.g., sandstones or limestones), fractured volcanic and crystalline rocks, etc. The rock contains water-filled pore spaces, and, when the spaces are connected, the water can flow through the matrix of the rock. Aquifers are categorized into four types as (i) confined, (ii) unconfined, (iii) perched, and (iv) leaky, which are having different storage capacities. Groundwater storage also encompasses a variety of chemical processes including dissolution, hydrolysis, and precipitation reactions, adsorption, and ion exchange. The major chemical components of groundwater are sodium ion, potassium ion, magnesium ion, calcium ion, bicarbonate ion, sulfate ion, chloride ion, and hydrogen silicate.

Groundwater studies are important for monitoring seasonal changes, demand assessment, targeting groundwater potential zones, and conservation. The traditional approaches for groundwater assessment use ground surveys employing geophysical, geological, and hydrogeological tools. However, such methods are time-consuming, are costly, and have scale limitation. However, the geospatial technique is an alternative approach that allows seasonal and long-term monitoring in the geographical area. The optical remote sensing system has a limitation in collecting data of the subsurface parameters; however, the suitable microwave sensors can penetrate surface soil layers enabling the proxy measure of the groundwater resource. The latest GRACE data measures the changes in the gravity field, which provides a proxy measure of groundwater storage. Rodell et al. (2009) analyzed the GRACE data and employed a hydrological model to simulate changes in groundwater storage and reported an annual depletion rate of  $4 \pm 1$  cm.year<sup>-1</sup> in Rajasthan, Punjab, and Haryana states of India.

Alternatively, the presence of groundwater can be inferred by integrating different proxy indicators on surface features derived from satellite imagery (i.e., land use land cover, surface water bodies, river network) and surveyed maps (i.e., geology, landforms, soils) (Todd 1980; Jha and Peiffer 2006). The assessment of groundwater potentiality using geospatial technology requires the study or integration of causative factors and field observations. Such factor mostly includes the layers as rainfall, topographic factors (slope, aspect), lithology, aquifer thickness, drainage density, lineaments, and land use land cover. The land utilization practice and vegetation cover play important roles in groundwater recharge processes (Leduc et al. 2001). The land slope determines the flow of water and residing time for water enabling groundwater recharge. The lower slope allows high groundwater recharge, while a higher slope leads to poor groundwater potential zones. Rainfall is one of the major sources for groundwater recharging through the hydrologic processes for a fractured aquifer (Ettazarini 2007). The soil texture regulates the percolation of water, where the fine-grained soil has lower permeability than coarse-grained. The sandy and coarse sandy clay soil are more suitable due to the higher infiltration rate that influences the groundwater recharge (Srivastava and Bhattacharya 2006), while clay soil is considered as poor due to being poorly drained, lower permeability, and hydraulic conductivity (Chowdhury et al. 2009).

The importance or influence of different data layers is either decided based on the expert's knowledge or derived through integrated analysis based on the field observed values. The obtained equation is then used to estimate values for other known location enabling validation of the developed model. Several methods have been adopted in various studies, i.e., analytical hierarchical process (AHP), frequency ratio (FR), multi-criteria decision analysis (MCDA), logistic regression (LR), decision tree (DT), and machine learning approaches as artificial neural network (ANN), Support Vector Machine (SVM), and random forest (RF) (Arulbalaji et al. 2019; Machiwal et al. 2011; Park et al. 2017; Duan et al. 2016; Lee et al. 2018; Naghibi et al. 2017). Shahid et al. (2000) adopted Analytical Hierarchy Process (AHP) method for assessing the groundwater potential zone deriving the Groundwater Potential Index (GWPI) based on seven factors, where

the existing borehole and pumping data was used to estimate the modeling accuracy. Gupta and Srivastava (2010) integrated various GIS layers on topography, geological structures, the extent of fractures, secondary porosity, slope, drainage pattern, landforms, LULC, and climatic conditions to estimate the groundwater potential in Pavagarh, Gujarat, India. Razandi et al. (2015) used FR and AHP to assess the groundwater potential zones, where they have followed three basic steps as (i) development of a spatial database on the various factors to regulate groundwater potential, (ii) spatial analysis of well locations and groundwater conditioning factors, and (iii) extrapolation and validation. Guru et al. (2017) assessed the groundwater potential zone in Leh valley using the FR model employing eight factors, including land use land cover map derived from LISS-IV data. For validation, the area under the curve was employed considering the cumulative percentage of spring wells and percent of groundwater potentiality index value. The FR model has been utilized in several studies for the demarcation of potential groundwater zones (Manap et al. 2013; Ozdemir 2011; Pourtaghi and Pourghasemi 2014).

Das et al. (2019) employed AHP and pair-wise comparison matrix to map the groundwater potential zone in Purulia district of West Bengal, India, and observed 60.92% and 16.53% of the study area under the moderate and lower potential zones. Chowdhury et al. (2009) delineated the groundwater potential zones in Paschim Medinipur (earlier Jhargram and Paschim Medinipur) employing the AHP technique and reported around 55% and 30% of the total area is residing in moderate and low potential zones. In the current study, we have demarcated the groundwater potential zones in two cropland- and forest-dominated districts as Jhargram and Paschim Medinipur, West Bengal, India, using the FR model.

## 10.2 Study Area

The Paschim Medinipur and Jhargram districts of West Bengal state are considered for the current study. The study regions are situated in the southern part of West Bengal. Geographically the area extension is in between latitude  $21^{\circ}45'39''\text{N}$  and  $22^{\circ}56'54''\text{N}$ , and longitude  $87^{\circ}53'20''\text{E}$  and  $86^{\circ}3'11''\text{E}$  falls under the Gangetic region (Fig. 10.1). The total area of the study region is 9393.15 km<sup>2</sup>. Agriculture is the predominant land use class followed by dense forest. The main three rivers in this region are as follows: Subarnarekha flows in the south part, the Kasai River flows in the heart of West Midnapore and Jhargram district, and the Silavati river creates a green stretch in the upper portion of the study area. The study region is classified as the sub-tropical climate zone. The mean annual precipitation is about 1560 mm, and the majority (~74%) of the precipitation occurs during the Monsoon, whereas the mean annual temperature varies from 9 °C in the winter to 44 °C in the summer.

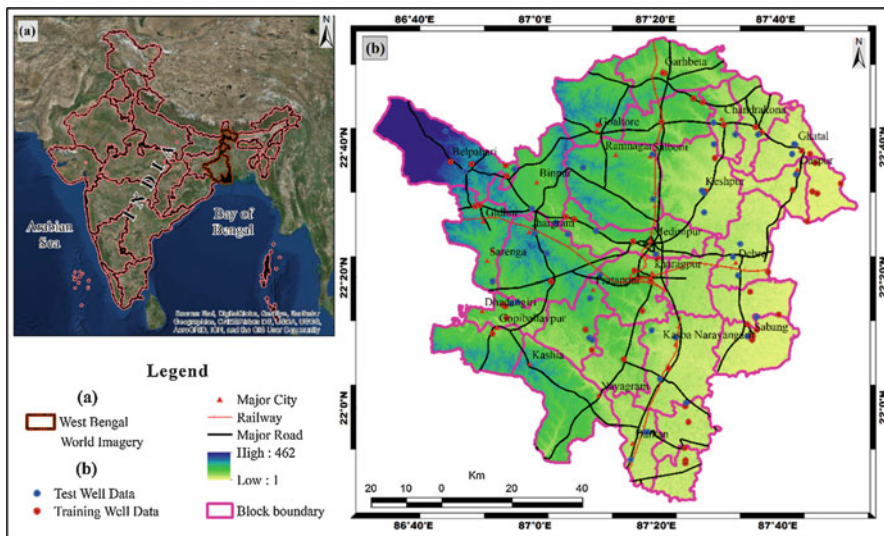


Fig. 10.1 Location map with SRTM elevation data of the study area

### 10.3 Data and Methodology

#### 10.3.1 Data Collection

For potential groundwater zones demarcation, various spatial layers are integrated into the current study. Sentinel-2 optical remote sensing data has been accessed from sentinel-hub portal to generate the land use land cover map and vegetation density map and identify the geomorphic units for the study area. The Shuttle Radar Topography Mission (SRTM) data derived digital elevation model (DEM; 30 m spatial resolution) is used to create the topographic variables (elevation and slope). The details of various other layers included in the current study are given in Table 10.1.

#### 10.3.2 Methodology

The Sentinel-2 bands having 10 m and 20 m spatial resolution were stacked to create the land use land cover map. The maximum likelihood classifier method was applied in the supervised classification, and the output map was verified with the high-resolution Google Earth imagery. The Sentinel-2 data is further used to derive the vegetation density map using the normalized difference vegetation index (NDVI). The SRTM DEM data is used to prepare the altitude map and derive the topographic slope map. The DEM data is further used for hydrological analysis to create the

**Table 10.1** Data used for identifying the groundwater potentiality

Data	Scale/ resolution	Source
Soil	1:250,000	National Bureau of Soil Survey and Land Use Planning (NBSS & LUP)
Geology	1:250,000	Geological Survey of India (GSI)
Geomorphological	1:50,000	The National Geomorphological and Lineament Mapping (NGLM)
Hydrogeology and well data	1:250,000	Central Groundwater Board (CGWB) and Geological Survey of India (GSI)
Rainfall	1 × 1 km	Climate Hazards Group InfraRed Precipitation with Station (CHIRPS) data
Lineament	1:50,000	The National Geomorphological and Lineament Mapping (NGLM)
Aquifer		India Water Resources Information System

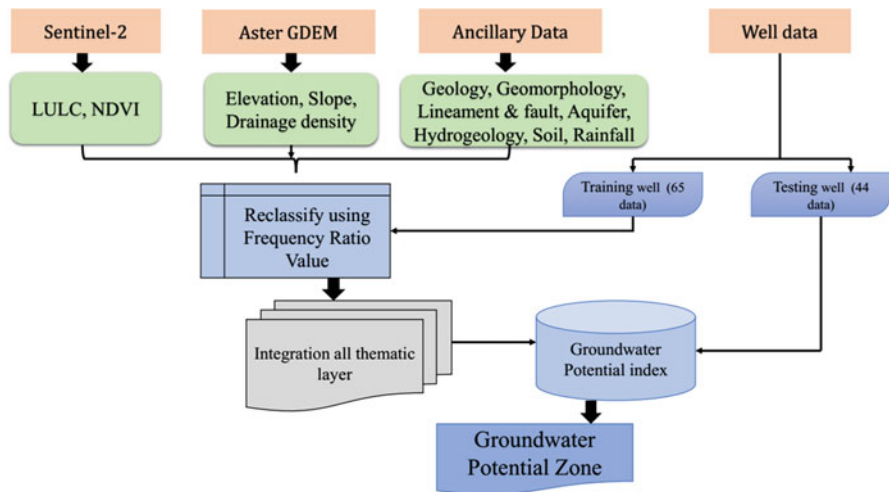


**Fig. 10.2** Overall methodology flowchart

stream or drainage network and corresponding density map. Similarly, the obtained lineament map is used to generate the lineament density map.

The frequency ratio (FR) method is used to estimate the groundwater potential. The FR method employs a bivariate statistical approach to determine the probabilistic relationship between the independent variables or factors and the dependent variable (Oh et al. 2011). Based on the literature survey, twelve important variables are selected, and corresponding criteria maps have been prepared. The selected criteria are elevation, slope, rainfall, drainage density, aquifer, geology, geomorphology, LULC, NDVI, soil, lineament density, and hydrogeology. The overall data analysis for groundwater potential zone mapping is depicted in Fig. 10.2. The FR is defined as the ratio of the area where groundwater wells (high groundwater

productivity) occurred in the total study area. FR model structure is based on the correlation and observed relationships between each groundwater conditioning factor and distribution of groundwater well locations. The following equation is used to compute the FR:

$$FR = \frac{W/G}{M/T} \quad (10.1)$$

where  $W$  is the number of pixels with groundwater well for each factor,  $G$  is the number of total groundwater wells in the study area,  $M$  is the number of pixels in the class area of the factor, and  $T$  is the number of total pixels in the study area.

Each map is then reclassified using the frequency ratio value, which was then overlaid to find out the Groundwater Potential Zone (GPZ) use the following equation:

$$GWPI = \sum_{R=1}^{R=n} FR \quad (10.2)$$

## 10.4 Results and Discussion

The details of the various thematic layers on land use land cover, vegetation, slope, altitude, rainfall, soil, geology, geomorphology, hydrogeology, drainage density, lineament density, and aquifer used in the current study are described as follows.

### 10.4.1 Land Use Land Cover (LULC)

Land use land cover (LULC) plays an important role in groundwater recharge. The Sentinel-2 data derived LULC map includes the classes as dense and open forest, agriculture fallow, cultivated land, settlement, sand, wetland, and water body (Fig. 10.3). The vegetation cover enables groundwater recharge via several ways as biological decomposition of the roots helps loosen the rock and soil and allows water to percolate the surface, while vegetation prevents runoff and direct evaporation of water from the soil. Moreover, the agriculture fallow (cultivated in monsoon season) and cultivated land enables groundwater recharge of the excess water standing on the ground.

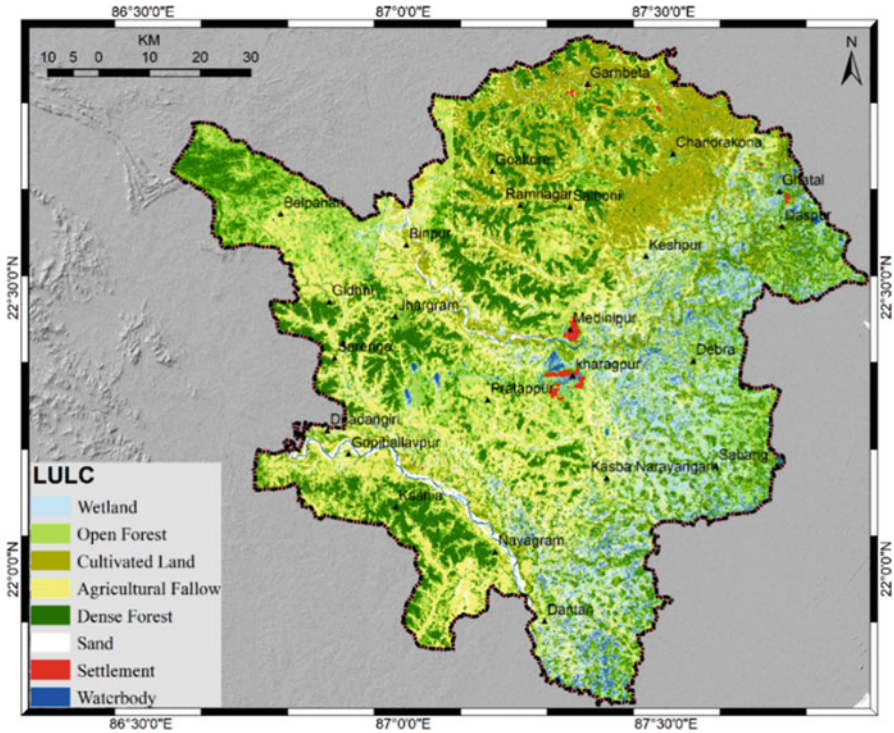


Fig. 10.3 Land use land cover (LULC) map of the study area

### 10.4.2 Vegetation

In addition to the LULC map, the Normalized Difference Vegetation Index (NDVI) map has been prepared using the red and NIR band of Sentinel 2 imagery to indicate the vegetation coverage in the terrain. The NDVI image was reclassified into five classes, where 0.16–0.24 indicates moderate vegetation density and the class with >0.24 NDVI values indicated dense vegetation and cropland during the post-monsoon rabi season (Fig. 10.4). However, the negative and low positive values indicated the water body and barren land areas. Dense vegetation is observed in the middle, the western, and upper parts of the region.

### 10.4.3 Altitude

The SRTM DEM data is used to prepare the altitude map indicating the height of any place from the datum. The altitude for the study area varies between 1 m and 462 m, where the altitude of the eastern part is observed lower than the western part. The



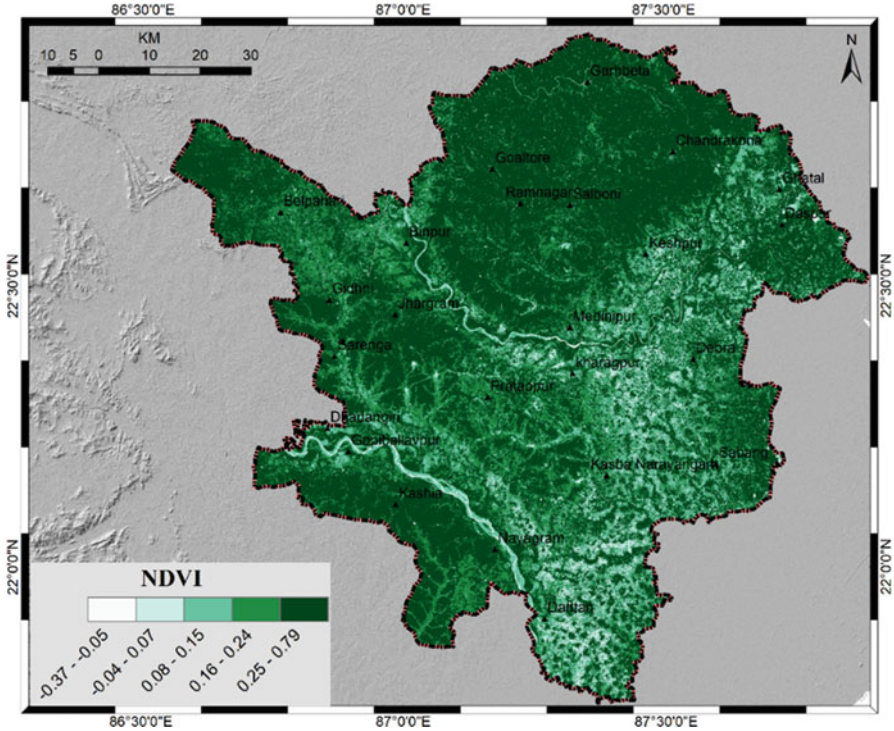
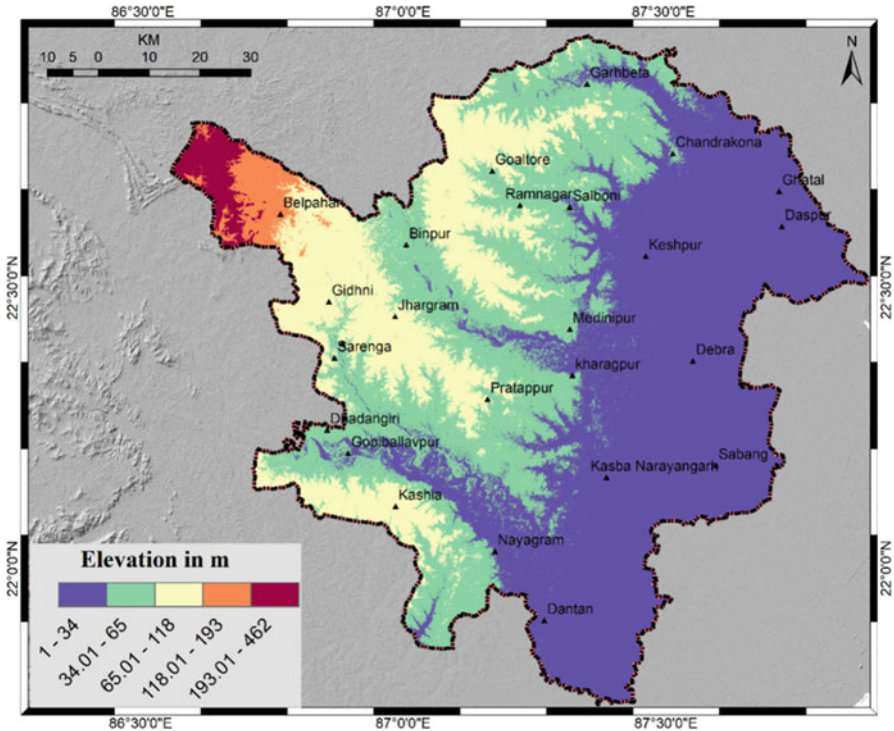


Fig. 10.4 Vegetation greenness map of the study area

altitude data is reclassified into five classes as 1–34 m, 34.01–65 m, 65.01–118 m, 118.01–193 m, and 193.01–462 m (Fig. 10.5).

### 10.4.4 Slope

Slope indicates the variations in topography and relates the local and regional relief setting, which determines the surface runoff and movement of water, and also regulates groundwater recharge. The observed slope (in degree) is divided into five classes as 0–2.33, 2.34–4.66, 4.67–7.58, 7.59–12.63, and 12.64–49.55 (Fig. 10.6). The majority of the study area belongs to the plain land where a few regions in the western part indicated a higher slope. The eastern part is dominated by alluvial plain, indicated a lower slope. On the other hand, the western part belongs to the hilly region with dominant gravels.



**Fig. 10.5** Altitude map of the study area

### 10.4.5 Rainfall

The annual rainfall and its seasonality are considered as one of the main factors of the hydrologic process that act as a source of groundwater recharge. The high-resolution satellite CHIRPS precipitation data integrated with the ground-based observations is used to prepare the annual rainfall map. The monthly rainfall range is divided into five classes as 170.00–178 mm, 178.01–188 mm, 188.01–193 mm, 193.01–198 mm, and 198.01–207.9 mm (Fig. 10.7). The relationship between rainfall distribution and well location indicated a positive correlation.

### 10.4.6 Soil

The soil layers regulate the percolation of water through pore spaces. The soil texture dominantly controls the infiltration of surface water into an aquifer, which is determined by the soil texture. The soil map at 1:25000 scale published by the National Bureau of Soil Survey and Land Use Planning (NBSS & LUP) is used in

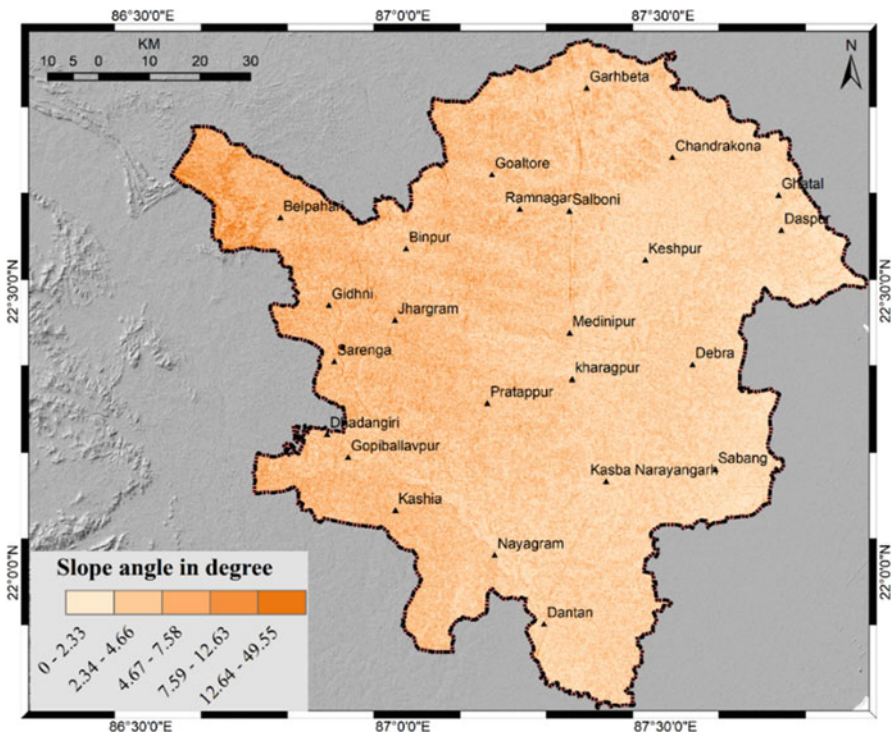


Fig. 10.6 Slope map of the study area, derived from Aster GDEM elevation data

the current study. The infiltration rate also depends on soil thickness and grain size. The coarse-grained soils have high permeability than fine-grained, such as sandy and coarse sandy clay. On the contrary, clay soil has low permeability and checks the groundwater recharge. The dominant soil types observed in this area are lateritic, older alluvial, red gravelly, red sandy, and younger alluvial (Fig. 10.8).

### 10.4.7 Geology

The type of rock exposed on earth’s surface plays an important role in groundwater recharge. Similar to the soil, the lithology also regulates the groundwater recharge by controlling the percolation of water. The geology map shown as Fig. 10.9 is accessed from the Geological Survey of India (GSI) indicating the occurrences of laterite and bauxite, Kuilpal granite, gravel and sandstone, Gangpur Gp, Dalma volcanic, coastal, and glacial sediments.

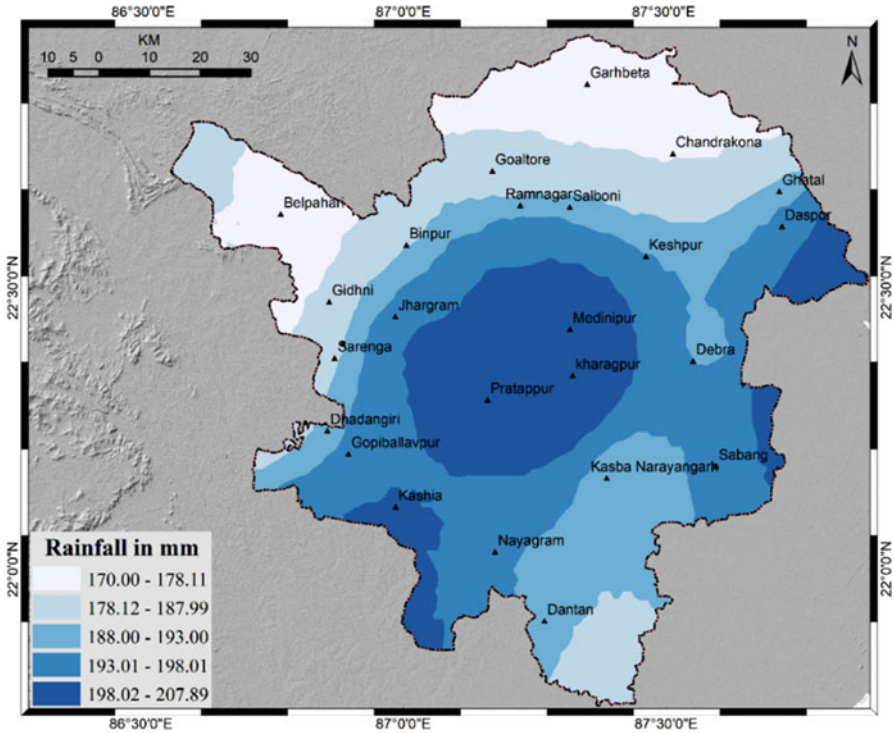


Fig. 10.7 Rainfall map of the study area

### 10.4.8 Geomorphology

The geomorphic features are indicated by the different landforms developed by the dynamic action of different geological processes as temperature change (freezing and thawing), chemical reactions, seismic shaking, and direction of wind and water (Ramaiah et al. 2012). The geomorphic features of the study area include (i) deep buried pediments, (ii) deep to moderately buried pediments with lateritic capping, (iii) denudational terrace and rocky outcrops, (iv) flood plain deposits, (v) moderately buried pediments with lateritic cropping, (vi) pediments, and (vii) valley fill deposits (Fig. 10.10).

### 10.4.9 Hydrogeology

Hydrogeology indicates the geological area that deals with the movement and redistribution of [groundwater](#). It regulates the water stored in aquifers and determines the pathways of flow and recharge. The different hydrogeological features

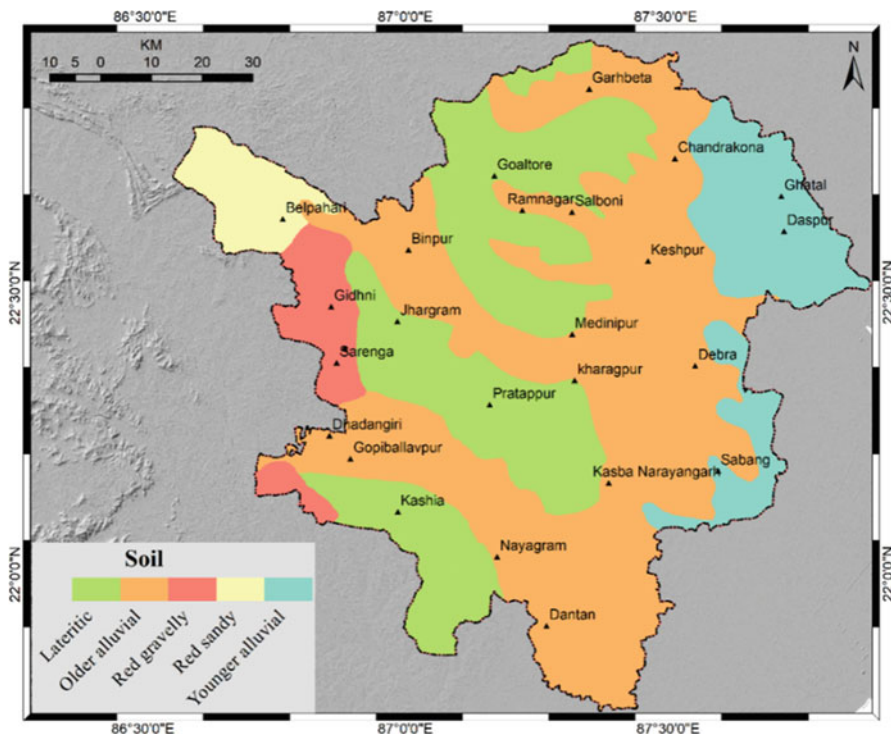
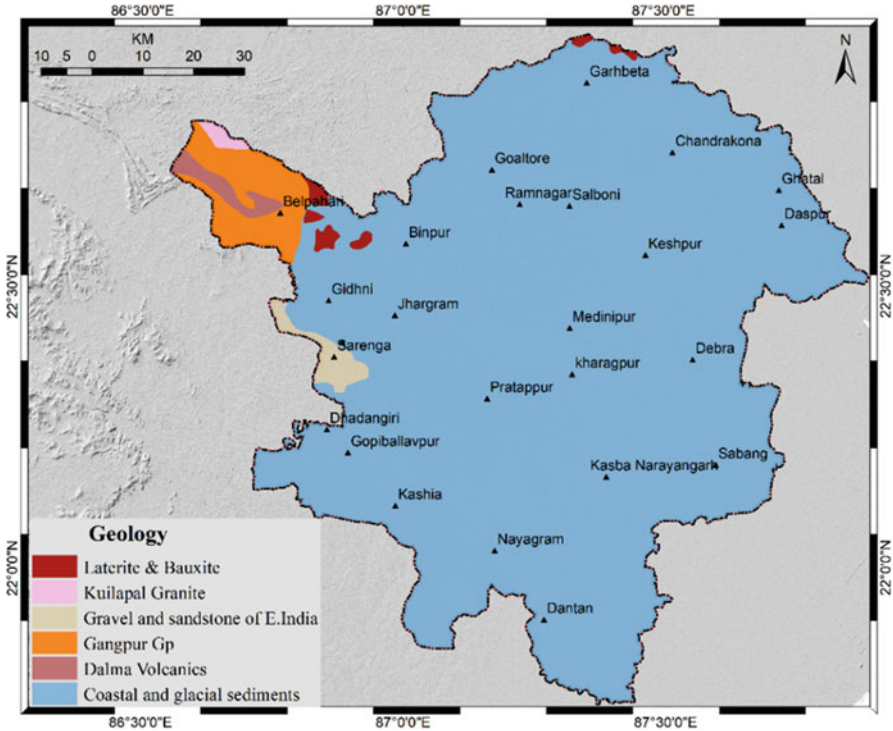


Fig. 10.8 Soil type map of the study area. (Source: NBSS & LUP)

present in the study area include quartz, phyllite, granite, pebbles, gravels, and sands with silts, clay impregnated with caliche nodules, etc., listed in Table 10.2 (Fig. 10.11).

#### 10.4.10 Drainage Density

The rate of groundwater recharge depends on the distribution of the drainage network. The stream network is a function of lithology and density function to the rate that rainfall or water infiltrates. Drainage density is inversely proportional to groundwater potential, where regions with high drainage density are unfavorable for groundwater existence, and, alternatively, regions with lower drainage density represent high groundwater potential zones. Low densities areas allow for longer



**Fig. 10.9** Geological map of the study area. (Source: GSI)

residence time, which allows the abstraction mechanisms to have more time to remove water (Gupta and Srivastava 2010). The drainage density is classified into five classes as 0–0.35, 0.36–0.55, 0.56–0.69, 0.70–0.83, and 0.84–1.19 (Fig. 10.12).

#### 10.4.11 Lineament Density

Lineaments are the structurally controlled linear or curvilinear features, enabling groundwater recharge through the fractures, fissures, joints, and faults (Sahoo et al. 2017). These features exhibit surface expression or topographic variations due to the underlying structural features and represent the potential zones of faulting and fracturing resulted from the increased secondary porosity and permeability. The lineaments are one of the most significant features in groundwater recharge which facilitate the pathways for groundwater flows. Lineament density is thus directly proportional to groundwater potential or recharge zones. The lineament data is accessed from the National Mission on Geomorphological and Lineament Mapping (NMGLM). The observed lineaments were used to generate the lineament density

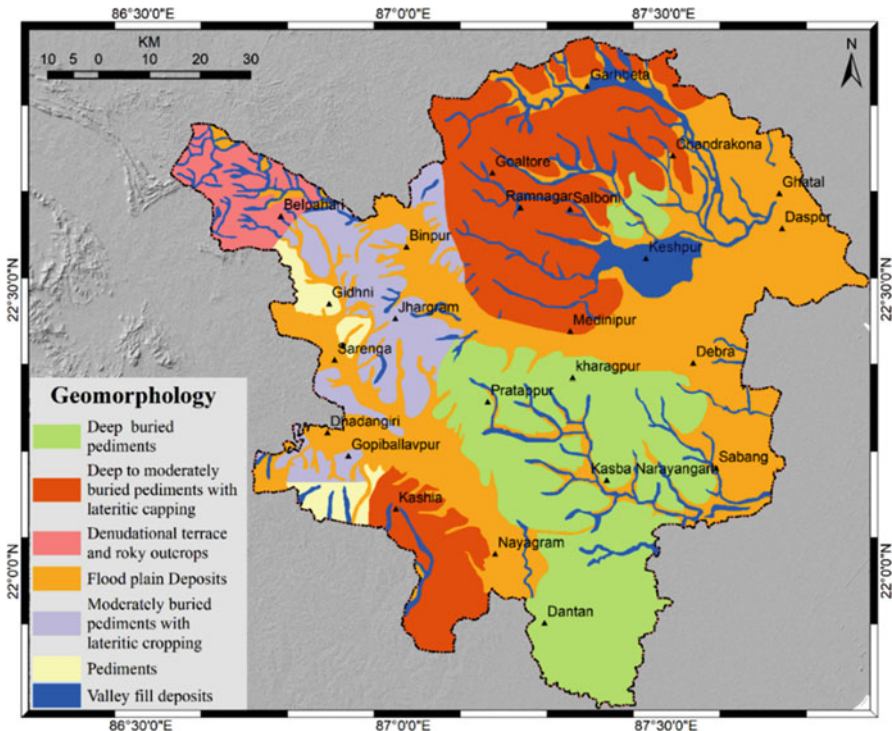
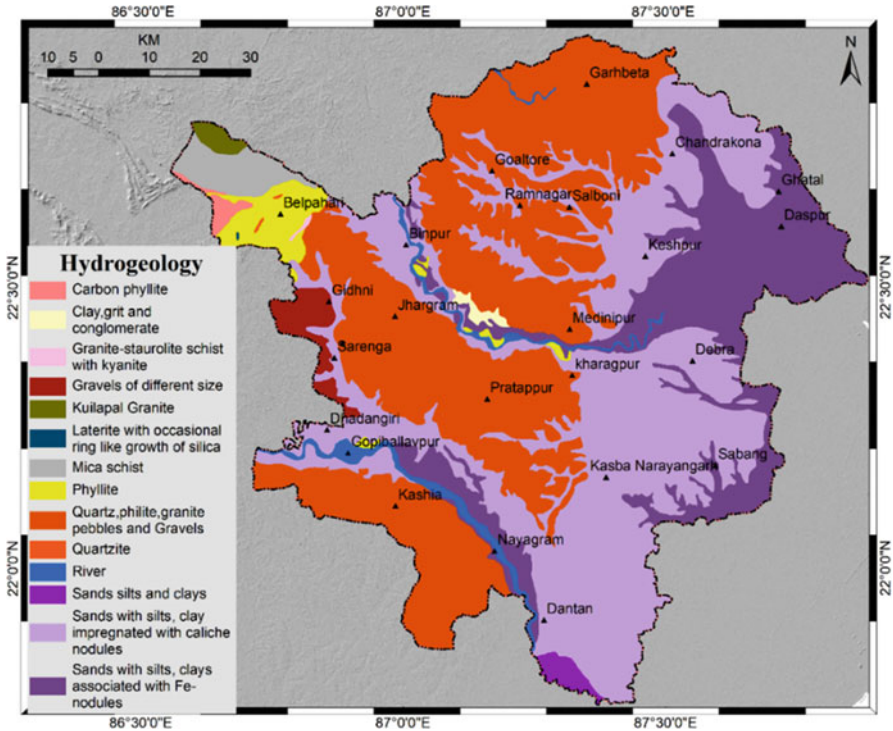


Fig. 10.10 Geomorphology map of the study area. (Source: NGLM)

Table 10.2 Hydrogeology classes and areas

Name	Area (km <sup>2</sup> )	Name	Area (km <sup>2</sup> )
Quart, phyllite, granite pebbles, and gravels	3639.81	Mica schist	167.98
Sands with silts, clays associated with Fe-nodules	1522.56	Carbon phyllite	37.36
Sands with silts, clay impregnated with caliche nodules	3379.52	Laterite with occasional ring-like growth of silica	0.80
River	161.71	Quartzite	2.86
Phyllite	222.83	Granite-staurolite schist with kyanite	4.63
Gravels of different size	123.54	Clay, grit, and conglomerate	26.64
Sands, silts, and clays	49.82	Sands with silts, clay impregnated with caliche nodules	14.67
Kuilapal granite	38.38		



**Fig. 10.11** Hydrogeology map of the study area. (Source: Central Groundwater Board (CGWB) and GSI)

map, which has been classified into five classes, viz., 0–0.03, 0.04–0.09, 0.1–0.15, 0.16–0.21, and 0.22–0.29 (Fig. 10.13).

**10.4.12 Aquifer**

An aquifer is an underground layer of water-bearing rock, where the permeable layers allow liquids and gasses to pass through, while the saturated permeable layers carry movable water and act as an instant groundwater source. Aquifer thickness is an important hydrogeological factor used to demarcate the groundwater potential zone. The four major aquifer systems are observed in the study area, viz., laterite, phyllite, schist, and younger alluvium, as depicted below in Fig. 10.14.

All the thematic layers were further reclassified using the frequency ratio method, which was further integrated to generate the groundwater potential zone for the study area. The calculation for the frequency ratio is shown in Table 10.3. The relation



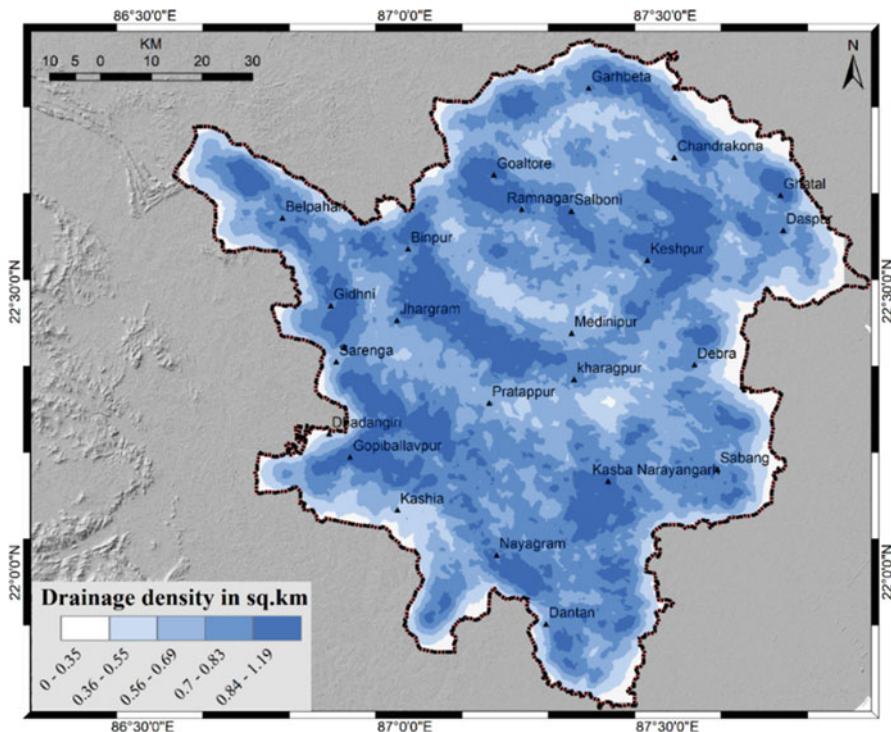
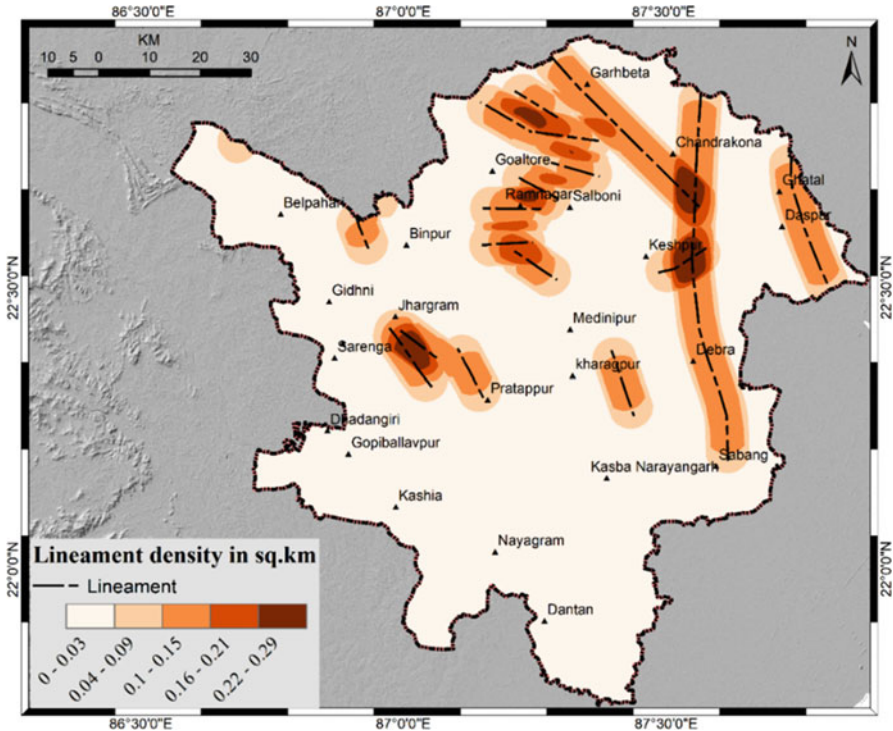


Fig. 10.12 Drainage density map of the study area

between percent (%) of class area, percent (%) of well in the class, and the frequency ratio (FR) value is shown as a line graph (Fig. 10.15).

The ROC curve is created by plotting the true-positive rate (TPR) against the false-positive rate (FPR) at various threshold settings. The true-positive rate indicates sensitivity, recall, or probability of detection. The obtained ROC curve indicated well-accepted accuracy of modeling (Fig. 10.16).

The groundwater potential zone map has been classified into four classes, viz., low, moderate, high, and very high potential zone. The eastern and central region of the study area is observed to have moderate and high groundwater potential covering ~40% and 30.15% of the total area, respectively. The lower potential zones observed in the north-west, west, and south-west regions cover 25.59% of the total area (Fig. 10.17). However, very high potential zones are observed in small patches in and around two major urban areas as Midnapore and Kharagpur city, including other urban areas. The number of wells per unit area is maximum for the very high groundwater potential zones having 14.68% (16 numbers) of the total wells. The majority of the wells around 44% (48 numbers) are observed in high potential zones,



**Fig. 10.13** Lineament density map of the study area. (Source: National Mission on Geomorphological and Lineament Mapping; NMGLM)

whereas 33% (36 numbers) of wells are observed in the moderate potential zone. The least number of wells at 8.26% (9 numbers) is observed in the low potential zone (Table 10.4). The dominant contributors to moderate and high potential zones include the geomorphology (flood plain deposit), alluvial soil layer, lower slope, hydrogeology (coarse texture sands with silt), and aquifer (younger alluvium). The estimated groundwater potential map and area statistics in the current study corroborates the similar studies carried out in this region by Chowdhury et al. (2009), where they have reported nearly similar distribution of moderate and good as well as poor potential zones. The majority of the areas as identified under the moderate and high potential zones indicate suitable zones, for artificial groundwater recharge zones as assessed by Chowdhury et al. (2010).

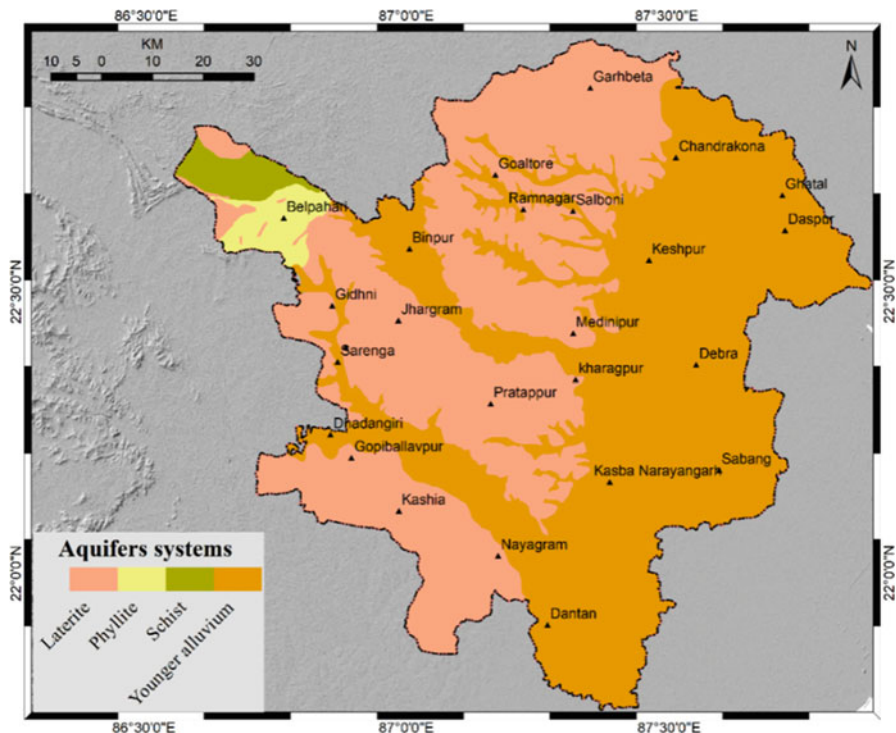


Fig. 10.14 Aquifer distribution of the study area. (Source: India WRIS)

### 10.5 Conclusion

The current study area is classified under the sub-tropical climate region, where the majority of the population is dependent on agriculture and the allied sector. Vast areas in these two districts are used for multiple cropping, where rice is cultivated in monsoon. On the contrary, the drier pre- and post-monsoon cropping (vegetables and cash crops) is primarily dependent on limited river and canal network for irrigation, while the groundwater is used for irrigation in the majority of the study area. Thus, assessment of groundwater potential is essential for the agriculture and water resource managers to adopt suitable measures ensuring the sustainable use of groundwater resources. For this, a number of factors are used, indicating the contributions of each theme and the sub-classes in estimating the groundwater potential zones for the study area. The dominant factors that lead to moderate and high potential zones include geomorphology, soil, slope, hydrogeology, and aquifer. The regions with flood plain deposits, dominated with alluvial coarse texture soil, located at a lower slope with younger alluvium aquifer, indicating moderate and high groundwater potential zones, were identified in around 40% and 30.15% of the area, respectively. The very high potential zones are identified in the minimal area in this

**Table 10.3** The calculation for frequency ratio

Attribute	Class	Class area	Class area %	No of wells	% of well	FR
<b>Aquifer</b>	Laterite	4,503,051	43.16	20	30.77	0.71
	Younger alluvium	5,528,807	52.99	42	64.62	1.22
	Phyllite	215,235	2.06	3	4.62	2.24
	Schist	186,653	1.79	0	0	0
<b>LULC</b>	Wetland	1,198,024	11.48	12	18.46	1.61
	Open forest	1,554,433	14.89	16	24.62	1.65
	Cultivated land	1,372,071	13.15	5	7.69	0.59
	Agricultural fallow	2,903,745	27.82	15	23.08	0.83
	Dense forest	2,592,458	24.84	12	18.46	0.74
	Sand	338,351	3.24	0	0	0
	Settlement	28,706	0.28	5	7.69	27.97
	Waterbody	448,995	4.3	0	0	0
<b>Geology</b>	Coastal and glacial sediments	9,840,211	94.31	63	96.92	1.03
	Gangpur Gp	463,885	4.45	2	3.08	0.69
	Laterite and bauxite	29,392	0.28	0	0	0
	Gravel and sandstone of E. India	100,594	0.96	0	0	0
<b>Geomorphology</b>	Deep buried pediments	2,315,682	22.19	15	23.08	1.04
	Denudational terrace and rocky outcrops	318,006	3.05	1	1.54	0.5
	Deep to moderately buried pediments with lateritic capping	2,249,177	21.55	7	10.77	0.5
	Valley fill deposits	928,096	8.89	6	9.23	1.04
	Flood plain deposits	3,596,672	34.46	32	49.23	1.43
	Pediments	215,714	2.07	0	0	0
	Moderately buried pediments with lateritic cropping	813,487	7.79	4	6.15	0.79
<b>Hydrogeology</b>	Quartz, phyllite, granite pebbles, and gravels	4,044,272	38.75	18	27.69	0.71
	Sands with silts, clays associated with Fe-nodules	1,691,678	16.21	14	21.54	1.33
	Sands with silts, clay impregnated with caliche nodules	3,770,279	36.13	30	46.15	1.28
	River	179,564	1.72	0	0	0
	Phyllite	247,639	2.37	2	3.08	1.3
	Gravel size	137,221	1.31	0	0	0
	Sand, silt, and clay	55,362	0.53	0	0	0
	Kuilapal granite	42,647	0.41	0	0	0
	Mica schist	186,653	1.79	0	0	0
	Carbon phyllite	41,503	0.4	0	0	0
	888	0.01	0	0	0	

(continued)

**Table 10.3** (continued)

Attribute	Class	Class area	Class area %	No of wells	% of well	FR
	Laterite with occasional ring-like growth of silica					
	Quartzite	3179	0.03	0	0	0
	Granite-staurolite schist with kyanite	5134	0.05	0	0	0
	Clay, grit, and conglomerate	29,615	0.28	1	1.54	5.42
<b>Lineament density</b>	0–0.03	7,667,175	73.46	41	63.08	0.86
	0.04–0.09	981,221	9.4	7	10.77	1.15
	0.10–0.15	1,371,136	13.14	15	23.08	1.76
	0.16–0.21	259,800	2.49	2	3.08	1.24
	0.22–0.29	157,472	1.51	0	0	0
<b>NDVI</b>	–0.32	50,390	0.48	0	0	0
	–0.11	366,678	3.51	4	6.15	1.75
	0.08–0.15	1,135,984	10.89	12	18.46	1.7
	0.16–0.24	2,440,609	23.39	12	18.46	0.79
	0.25–0.79	6,441,774	61.73	37	56.92	0.92
<b>Soil</b>	Red sandy	453,869	4.35	1	1.54	0.35
	Red gravelly	501,765	4.81	2	3.08	0.64
	Lateritic	3,140,607	30.09	10	15.38	0.51
	Older alluvial	5,063,651	48.52	35	53.85	1.11
	Younger alluvial	1,276,918	12.23	17	26.15	2.14
<b>Drainage Density</b>	0.02–0.52	813,992	7.8	3	4.62	0.59
	0.53–0.73	1,884,140	18.05	11	16.92	0.94
	0.74–0.87	3,583,328	34.33	16	24.62	0.72
	0.88–1.02	3,202,668	30.69	31	47.69	1.55
	1.03–1.64	952,676	9.13	4	6.15	0.67
<b>Slope</b>	0–2.33	3,578,823	34.29	29	44.62	1.3
	2.34–4.66	4,156,950	39.83	22	33.85	0.85
	4.67–7.58	1,963,869	18.82	12	18.46	0.98
	7.59–12.63	639,984	6.13	2	3.08	0.5
	12.64–49.55	96,707	0.93	0	0	0
<b>Altitude</b>	<34	4,903,794	46.99	37	56.92	1.21
	34.01–65	3,172,837	30.4	20	30.77	1.01
	65.01–118	1,945,785	18.64	7	10.77	0.58
	118.01–193	224,476	2.15	1	1.54	0.72
	193.01–462	189,441	1.82	0	0	0
<b>Rainfall</b>	170.00–178.11	406,590	3.9	2	3.08	0.79
	178.12–187.99	2,939,568	28.17	18	27.69	0.98
	188.00–193.00	1,935,041	18.54	7	10.77	0.58
	193.01–198.01	1,319,452	12.64	12	18.46	1.46
	198.02–207.89	3,835,114	36.75	26	40	1.09

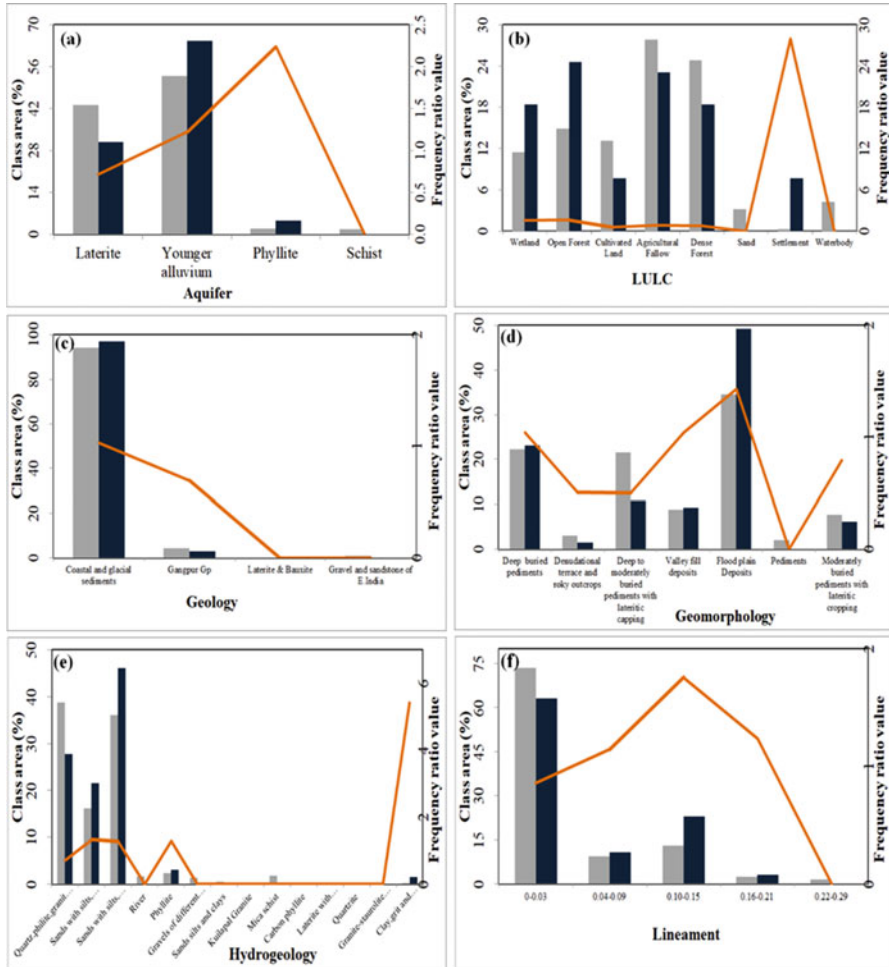


Fig. 10.15 Frequency ratio plot of different parameters

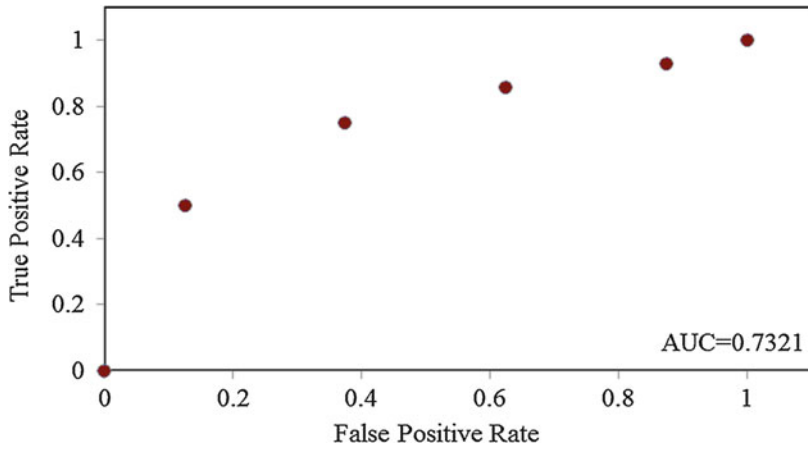


Fig. 10.16 ROC curve showing the false-positive rate with true-positive rate

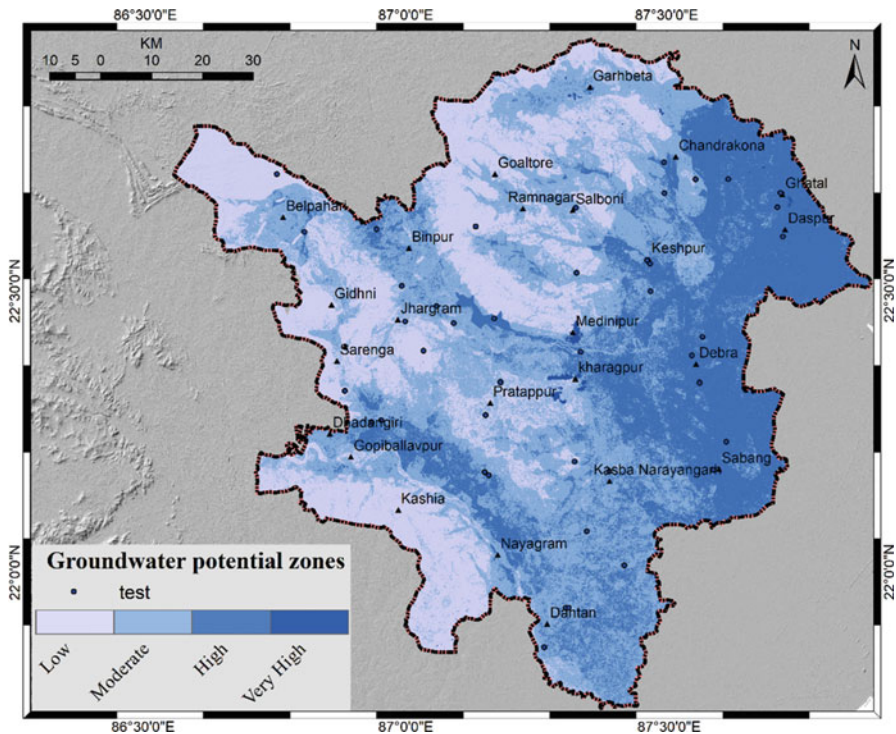


Fig. 10.17 Groundwater potential zone map of the study area

**Table 10.4** Area statistics of potentiality map

Class	Area	% Area	No. of well
Low	2780	29.59	9
Moderate	3755	39.98	36
High	2832	30.15	48
Very high	26	0.8	16
<b>Total</b>	9393		109

region, mostly observed in and around the two major cities as Midnapore and Kharagpur. The accuracy as observed from the ROC curve specified the consistency of the frequency ratio method in demarcating groundwater zones. The obtained spatial map also corroborates similar studies in this region, where the moderate and high potential zones indicated a higher potential for artificial groundwater recharge.

## References

- Arulbalaji, P., Padmalal, D., & Sreelash, K. (2019). GIS and AHP techniques based delineation of groundwater potential zones: a case study from southern Western Ghats, India. *Scientific reports*, 9(1), 1–17.
- Asoka, A., Gleeson, T., Wada, Y., & Mishra, V. (2017). Relative contribution of monsoon precipitation and pumping to changes in groundwater storage in India. *Nature Geoscience*, 10 (2), 109–117.
- Chowdhury, A., Jha, M. K., & Chowdary, V. M. (2010). Delineation of groundwater recharge zones and identification of artificial recharge sites in West Medinipur district, West Bengal, using RS, GIS and MCDM techniques. *Environmental Earth Sciences*, 59(6), 1209.
- Chowdhury, A., Jha, M. K., Chowdary, V. M., & Mal, B. C. (2009). Integrated remote sensing and GIS-based approach for assessing groundwater potential in West Medinipur district, West Bengal, India. *International Journal of Remote Sensing*, 30(1), 231–250.
- Das, B., Pal, S. C., Malik, S., & Chakraborty, R. (2019). Modeling groundwater potential zones of Purulia district, West Bengal, India using remote sensing and GIS techniques. *Geology, Ecology, and Landscapes*, 3(3), 223–237.
- Duan, H., Deng, Z., Deng, F., & Wang, D. (2016). Assessment of groundwater potential based on multicriteria decision making model and decision tree algorithms. *Mathematical Problems in Engineering*, 2016.
- Ettazarini, S. (2007). Groundwater potentiality index: a strategically conceived tool for water research in fractured aquifers. *Environmental Geology*, 52(3), 477–487.
- Groundwater Yearbook 2013–14, July 2014, Central Groundwater Board. Govt. of India.
- Gupta, M., & Srivastava, P. K. (2010). Integrating GIS and remote sensing for identification of groundwater potential zones in the hilly terrain of Pavagarh, Gujarat, India. *Water International*, 35(2), 233–245.
- Guru, B., Seshan, K., & Bera, S. (2017). Frequency ratio model for groundwater potential mapping and its sustainable management in cold desert, India. *Journal of King Saud University-Science*, 29(3), 333–347.
- <http://india-wris.nrsc.gov.in/LithologApp.html?UType=R2VuZXJhbA==?UName = 08 may 2018>
- <https://www.un-igrac.org/what-groundwater> 17/04/2018



- Jha, M. K., & Peiffer, S. (2006). Applications of remote sensing and GIS technologies in groundwater hydrology: past, present and future (p. 201). Bayreuth: BayCEER.
- Leduc, C., Favreau, G., & Schroeter, P. (2001). Long-term rise in a Sahelian water-table: The Continental Terminal in south-west Niger. *Journal of hydrology*, 243(1–2), 43–54.
- Lee, S., Hong, S. M., & Jung, H. S. (2018). GIS-based groundwater potential mapping using artificial neural network and support vector machine models: the case of Boryeong city in Korea. *Geocarto international*, 33(8), 847–861.
- Machiwal, D., Jha, M. K., & Mal, B. C. (2011). Assessment of groundwater potential in a semi-arid region of India using remote sensing, GIS and MCDM techniques. *Water resources management*, 25(5), 1359–1386.
- Manap, M. A., Sulaiman, W. N. A., Ramli, M. F., Pradhan, B., & Surip, N. (2013). A knowledge-driven GIS modeling technique for groundwater potential mapping at the Upper Langat Basin, Malaysia. *Arabian Journal of Geosciences*, 6(5), 1621–1637.
- Naghbi, S. A., Ahmadi, K., & Daneshi, A. (2017). Application of support vector machine, random forest, and genetic algorithm optimized random forest models in groundwater potential mapping. *Water Resources Management*, 31(9), 2761–2775.
- Oh, H. J., Kim, Y. S., Choi, J. K., Park, E., & Lee, S. (2011). GIS mapping of regional probabilistic groundwater potential in the area of Pohang City, Korea. *Journal of Hydrology*, 399(3–4), 158–172.
- Ozdemir, A. (2011). GIS-based groundwater spring potential mapping in the Sultan Mountains (Konya, Turkey) using frequency ratio, weights of evidence and logistic regression methods and their comparison. *Journal of Hydrology*, 411(3–4), 290–308.
- Pandey, V., & Srivastava, P. K. (2019). Integration of microwave and optical/infrared derived datasets for a drought hazard inventory in a sub-tropical region of India. *Remote Sensing*, 11(4), 439.
- Park, S., Hamm, S. Y., Jeon, H. T., & Kim, J. (2017). Evaluation of logistic regression and multivariate adaptive regression spline models for groundwater potential mapping using R and GIS. *Sustainability*, 9(7), 1157.
- Pourtaghi, Z. S., & Pourghasemi, H. R. (2014). GIS-based groundwater spring potential assessment and mapping in the Birjand Township, southern Khorasan Province, Iran. *Hydrogeology Journal*, 22(3), 643–662.
- Ramaiah, S. N., Gopalakrishna, G. S., Vittala, S. S., & Najeeb, K. M. (2012). Geomorphological Mapping for Identification of Ground Water Potential Zones in Hard Rock Areas Using Geospatial Information-A Case Study in Malur Taluk, Kolar District, Karnataka, India. *Nature Environment and Pollution Technology*, 11(3), 369.
- Razandi, Y., Pourghasemi, H. R., Neisani, N. S., & Rahmati, O. (2015). Application of analytical hierarchy process, frequency ratio, and certainty factor models for groundwater potential mapping using GIS. *Earth Science Informatics*, 8(4), 867–883.
- Rodell, M., Velicogna, I., & Famiglietti, J. S. (2009). Satellite-based estimates of groundwater depletion in India. *Nature*, 460(7258), 999–1002.
- Saha, D., & Ray, R. K. (2019). Groundwater resources of India: Potential, challenges and management. In *Groundwater Development and Management* (pp. 19–42). Springer, Cham.
- Sahoo, S., Munusamy, S. B., Dhar, A., Kar, A., & Ram, P. (2017). Appraising the Accuracy of Multi-Class Frequency Ratio and Weights of Evidence Method for Delineation of Regional Groundwater Potential Zones in Canal Command System. *Water Resources Management*, 31(14), 4399–4413.
- Shahid, S., Nath, S., & Roy, J. (2000). Groundwater potential modelling in a soft rock area using a GIS. *International Journal of Remote Sensing*, 21(9), 1919–1924.
- Srivastava, P. K., & Bhattacharya, A. K. (2006). Groundwater assessment through an integrated approach using remote sensing, GIS and resistivity techniques: a case study from a hard rock terrain. *International Journal of Remote Sensing*, 27(20), 4599–4620.

- Teixeira, J., Chaminé, H. I., Carvalho, J. M., Pérez-Alberti, A., & Rocha, F. (2013). Hydrogeomorphological mapping as a tool in groundwater exploration. *Journal of Maps*, 9 (2), 263–273.
- Todd, D. K. (1980). *Groundwater Hydrogeology* ed. 2nd. John Willey and Sons, New York, 537.
- WRI India report, 2015: <https://www.wri.org/blog/2015/02/3-maps-explain-india-s-growing-water-risks>; visited on 20/09/2020